A Signal Decomposition Algorithm Based on Multiple Complex AMFM Model

De Zhu[1] · Qingwei Gao[2] · Yixiang Lu[2] · Dong Sun[2]

Abstract

The model-based signal decomposition algorithm is an important research direction in the field of digital signal processing, especially based on the amplitude modulation and frequency modulation (AMFM) model. In this paper, a signal decomposition algorithm based on multiple complex AMFM model is proposed to analyze multi-model data sets. Firstly, the analyzed signal is converted into the form of the analytic signal because of the simple representation of the AMFM model in the analytic domain. Then, the multi-model optimization equation of the analytic signal is realized by the estimated instantaneous frequency (IF) of each model, which can be estimated by time–frequency analysis (TFA). Finally, each model parameter of the optimization equation is solved by the partial differential equation and the alternating direction method of multipliers method (ADMM) to find the global optimal solution of the signal. In the optimization equation, we introduce the leakage factor to improve the extraction accuracy of the model; at the same time, we employ the cyclic iteration method to optimize the equation parameters to improve the convergence rate of the algorithm. Several examples of the simulated and real-life signals are provided to show that the proposed algorithm can accurately estimate the parameters of each model in the signal.

Keywords Signal processing · Time–frequency analysis · Adaptive model decomposition · Complex AMFM model · Nonlinear multi-component signal

✉ Qingwei Gao
  qingweigao@ahu.edu.cn

Extended author information available on the last page of the article

1 Introduction

The description and expression of signals have always been an important research topic in the field of signal research. The premise of accurately expressing the signal is to master the composition of the signal. The widely accepted idea of signal decomposition methods is to decompose the signal into the sum of a series of simple signals. The simple signal here can be a single expression of a component in a certain frequency domain or some signal model with special properties.

In the past decades, a large number of signal decomposition algorithms have been proposed. We know that the fast Fourier transform (FFT) successfully transforms the time domain signal to the frequency domain, which plays a milestone role in the development of modern digital signal processing [23]. Then, the short-time Fourier transform (STFT) [20] is proposed, which can reflect the time-varying characteristics of the signal. Wavelet transform (WT) introduces the concept of scale based on STFT to effectively show the time–frequency characteristics of the signal [8]. To improve the resolution of the instantaneous frequency (IF) of components in WT, the synchrosqueezed wavelet transforms (SST) algorithm was proposed, which uses an energy redistribution method to provide the time–frequency representation of the signals [7].

The synchroextracting transform (SET) is inspired by SST and the ideal time–frequency analysis, designed to improve the energy concentration of the time–frequency analysis while retaining only the time–frequency information related to the time-varying characteristics of the signal [31]. To further improve the energy concentration of the signal to adapt to different application scenarios, multiple SST-based improved algorithms have been proposed [22, 25, 30]. Although this kind of algorithm ensures the maximum energy in the frequency domain of the signal, it may also destroy the model structure of the signal because this kind of algorithms completely ignores the characteristics of the signal model.

The empirical mode decomposition (EMD) [3, 18] is a purely data-driven signal decomposition algorithm that expresses the signal as the sum of a series of the Intrinsic Mode Function (IMF) models. At the later stage, some scholars put forward some important improved algorithms based on the EMD algorithm, such as the ensemble empirical mode decomposition (EEMD) [28], the complementary ensemble empirical mode decomposition (CEEMD) [29], and so on. These methods demonstrate excellent ability in analyzing nonlinear and nonstationary signals. Unfortunately, EMD lacks rigorous mathematical derivation and has the problem of model aliasing.

Then, K. Dragomiretskiy proposed the variational mode decomposition (VMD) algorithm [11], which draws on both spectrum and signal model features. According to the number of models to be decomposed, the algorithm divides the spectrum into several frequency bands to find the optimal model parameters. Later, a series of improved and extended algorithms based on VMD were proposed [10, 24, 27]. However, this kind of algorithms cannot extract the model with the frequency crossover [19].

Besides, the signal decomposition algorithm based on other signal models is also studied and proposed by some scholars. Chen proposed a signal decomposition algorithm based on the Chirp model, for example, which has achieved good decomposition results [4, 6]. This kind of algorithm uses the IF of the signal model to find the optimal solution of the model through the cycle iteration of the optimization equation. However, this kind of algorithm is only suitable for detecting the Chirp model with slower fluctuation.

In addition, operator-based signal decomposition algorithms have also been proposed and received extensive attention [21]. It can design the corresponding operators according to different signal models and then realize the multi-model decomposition of the signal by solving the optimization equation of the model [14–17]. At the same time, this kind of algorithm is applied in signal noise reduction, bearing fault diagnosis, and other fields [13, 33, 34].

The amplitude modulation and frequency modulation (AMFM) model is one of the most common signal models in natural and artificial systems and one of the signal models widely studied and used. An adaptive signal decomposition algorithm based on a complex AMFM model (ASD-CAMFM) has been proposed, which can decompose the signal into multiple single components in turn [32]. However, this algorithm has a poor effect on the detection of signals with frequency crossover.

In this paper, an adaptive signal decomposition algorithm based on the multi-model is proposed by analyzing the AMFM model characteristics of the complex domain. The proposed algorithm can decompose the signal into the sum of several AMFM models and estimate the parameters of each model accurately. This algorithm also has high decomposition accuracy for signals with frequency crossover.

The remainder of this paper is organized as follows. Section 2 describes the mathematical model and review of the single component decomposition algorithm based on the model. Section 3 introduces the algorithm principle and implementation process in detail. The performance of the proposed algorithm is verified by experimental including the simulated and real-life signals in Sect. 4, and the conclusion is presented in Sect. 5.

2 Background

2.1 Signal Model

In general, a multicomponent signal can be regarded as a superposition of multiple components, which conform to some kind of mathematical model. This paper mainly analyzes the estimation of the AMFM model, which is defined as follows:

$$s(t) = a(t) \cos(2\pi f(t)t + \theta), \tag{1}$$

where $a(t)$ is instantaneous amplitude (IA) of $s(t)$, $f(t)$ is IF of $s(t)$ and θ is the initial phase. We define $f_a(t)$ is IF of $a(t)$. In addition, the model satisfies the following conditions:

(1) $a(t)$ and $f(t)$ have continuous derivatives.
(2) Both $a(t)$ and $f(t)$ are non-negative.
(3) $f_a(t) << f(t)$ and $f'(t) << f(t)$.

According to the theory of Hilbert Transform (HT) [2], the analytic expression of $s(t)$ can be obtained by HT as follows:

$$\begin{aligned} s_A(t) &= s(t) + j \cdot s_H(t) \\ &= a(t) \exp{(j2\pi f(t)t + \theta)}, \end{aligned} \qquad (2)$$

where $s_H(t)$ is HT of $s(t)$.

The signal $x(t)$ consisting of several AMFM components is expressed as follows:

$$x(t) = \sum_{k=1}^{K} s_k(t), \quad \text{with} \quad s_k(t) = a_k(t) \cos(2\pi f_k(t)t + \theta_k), \qquad (3)$$

where $x(t)$ is composed of K components $s_k(t)$, which fully conform to the characteristics of the AMFM model.

We can get the analytic expressions of $x(t)$ by HT, as follows:

$$x_A(t) = \sum_{k=1}^{K} s_{k_A}(t), \qquad (4)$$

where $s_{k_A}(t)$ is the analytic expression of $s_k(t)$.

2.2 Signal Decomposition Algorithm of Single Model

The common idea of the model-based signal decomposition algorithm is to decompose the signal into the sum of several models through cyclic iteration, which extracts one model at a time. Such as EMD [18], VMD [11], ACMP [6] and ASD-CAMFM [32] all belong to this kind of algorithms. These algorithms have a good decomposition effect for the signal without spectral overlap, but when analyzing the signal with frequency crossover, they will produce a certain detection error in the range of cross-spectrum. Here, we use ASD-CAMFM as an example to introduce and analyze.

ASD-CAMFM is an optimization algorithm for signal decomposition based on complex-AMFM model [32]. We set the signal $x(t) = a(t) \cos(2\pi f(t)t + \theta)$, which satisfy the above model. Its analytic form is $x_A(t) = a(t) \exp(j2\pi f(t)t + \theta)$. We need to estimate the IF ($\hat{f}(t)$) of the model by SET or STFT, and then we can estimate the model parameters by calculating the following optimization problems:

$$\begin{aligned} &\min_{\{P(t), \hat{f}(t)\}} \left\{ \|T(P(t))\|_2^2 \right\}, \\ &s.t. \ \left\| x_A(t) - P(t) \cdot Q(t) \right\|_2^2 \leq \varepsilon, \end{aligned} \qquad (5)$$

where $P(t) = a(t) \exp\left(j2\pi\left(\hat{f}(t) - f(t)\right)t\right)$, $Q(t) = \exp\left(j2\pi\hat{f}(t)t + \theta\right)$, ε is the upper bound of the estimated residue, T is a differential operator. Then the above optimization problem is transformed into the following Lagrange polynomial solution problem:

$$\Gamma(P, Q) = \|T(P(t))\|_2^2 + \lambda(\|P(t) * Q(t)(1 + \upsilon) - x_A(t)\|_2^2), \tag{6}$$

where λ is the Lagrange multiplier and υ is the leak factor.

The following iterative formula of $P(t)$ is obtained by the partial derivative of (6):

$$P_i(t) = \left(\frac{T^H T}{\lambda} + Q_i(t)^H Q_i(t)(1 + \upsilon)\right)^{-1} Q_i(t)^H(1 + \upsilon)x_A(t). \tag{7}$$

By cyclic iteration, this algorithm decomposes the signal into the form of the sum of several AMFM models. To illustrate the problem, we define a signal as follows:

$$x(t) = x_1(t) + x_2(t),$$
$$x_1(t) = (1 + 0.2sin(2\pi \cdot 0.6t)) \cdot sin(2\pi \cdot (60t + 15t^2 + 5sin(1.2t))), \tag{8}$$
$$x_2(t) = (0.2 + \exp(-0.8t)) \cdot sin(2\pi \cdot (130t + 2sin(2.5t))).$$

The signal consists of two components, and the information of the signal is shown in Fig. 1. From Fig. 1b, it can be seen that the IAs and IFs of the two components vary with time, and they intersect at a frequency of 134.8 Hz at 2.6 s.

We sequentially extract $x_2(t)$ and $x_1(t)$ from the signal (8) by ASD-CAMFM, and extracted results are shown in Fig. 2. From Fig. 2, it can be seen that the estimated IF of $x_2(t)$ is acceptable by the algorithm, but the estimated IA of $x_2(t)$ has a clear error around 2.6 s. At the same time, the estimated IA and IF of $x_1(t)$ have a large estimation error around 2.6 s.
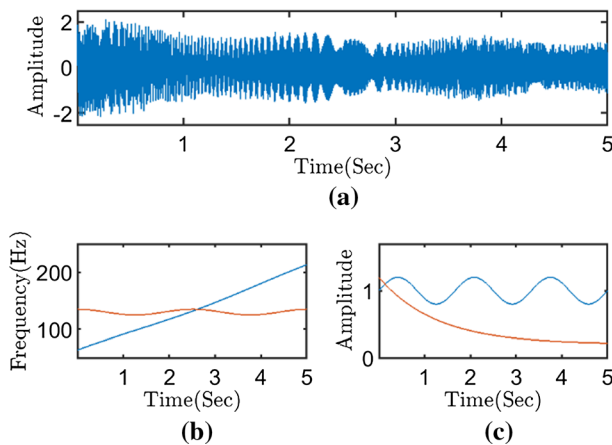

Fig. 1 Information of the artificial signal (8). **a** Waveform of the $x(t)$; **b** IFs of two components in signal; **c** IAs of two components in signal (red line: information of $x_1(t)$, blue line: information of $x_2(t)$) (Color figure online)
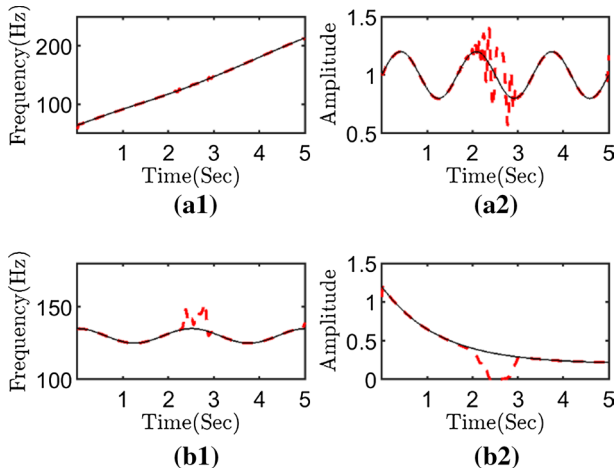
Fig. 2 Extracted results of the signals (8) by ASD-CAMFM. **a** Estimated IF and IA of $x_2(t)$; **b** estimated IF and IA of $x_1(t)$

We analyze the causes of the estimation errors. When the algorithm extracts the first component of the signal, the IF of the extracted component can be accurately estimated, and the IA corresponding to the IF is also effectively separated. Thus, it leads to the IA of the intersection point is almost zero at the second extraction and the IF at the intersection point has a large estimation error. We will introduce how to solve such problems by a multi-model decomposition algorithm in the following section.

3 Proposed Algorithm

According to Sect. 2.2, when using ASD-CAMFM to analyze multiple component signals, the algorithm extracts the IF of a single component and the total energy in the frequency domain of the component. This may break the integrity of the residual components of the signal. That is to say, this kind of algorithm only realizes the optimal solution of the component and the remaining component, not the optimal solution of all components and the noise component.

In this section, we mainly introduce the signal decomposition algorithm based on the multi-model. In addition, we will analyze in detail how to avoid the estimation error problem in the cross-frequency part.

3.1 Algorithm Principle

If we need to solve the optimal solution of each component and the residue, we must modify the optimization equation, which should contain all the components. For signals composed of multiple components, such as (4), if $\hat{f}_k(t)$ is the estimated IF of $s_{k_A}(t)$. Therefore, we can get the following signal representation:

$$x_A(t) = \sum_{k=1}^{K} a_k(t) \exp\left(j2\pi(f_k(t))t + \theta_k\right)$$

$$= \sum_{k=1}^{K} a_k(t) \exp\left(j2\pi(f_k(t) - \hat{f}_k(t))t\right) \exp(j2\pi\hat{f}_k(t)t + \theta_k) \tag{9}$$

$$= \sum_{k=1}^{K} P_k(t)Q_k(t)$$

where $P_k(t) = a_k(t) \exp\left(j2\pi(f_k(t) - \hat{f}_k(t))t\right)$ and $Q_k(t) = \exp\left(j2\pi\hat{f}_k(t)t + \theta_k\right)$.

When $\hat{f}_k(t)=f_k(t)$, then $P_k(t) = a_k(t)$ and $Q_k(t) = \exp\left(j2\pi f_k(t)t+\theta_k\right)$. Thus $s_{k_A}(t)=P_k(t)Q_k(t)$. So, we can divide the AMFM model into the form of multiplying the AM component with the FM component.

The concept of instantaneous bandwidth (IB) is proposed in [14], which means that the signal occupies a certain band bandwidth during transmission. From the perspective of IB, the IB of AMFM signal is mainly reflected in two parts: bandwidth characteristic of AM and bandwidth characteristic of FM. Meanwhile, the IB of the AMFM model can be represented in the form of the sum of these two bandwidths, shown in Fig. 3.

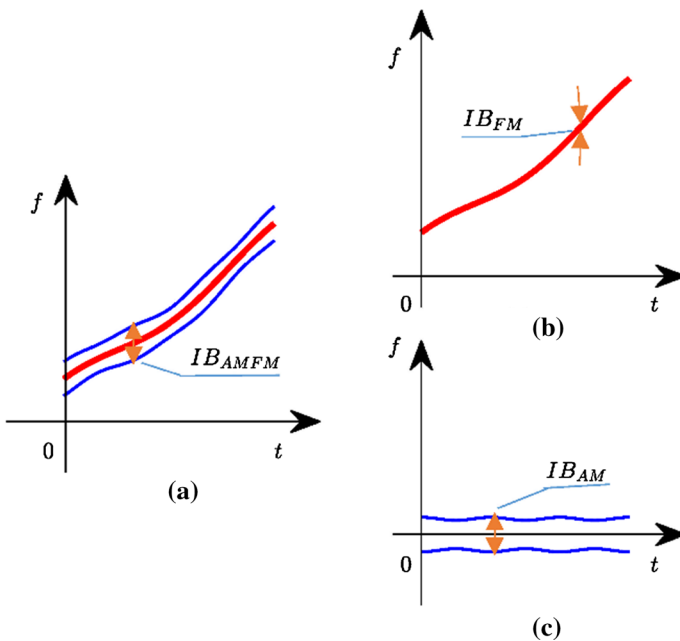$$IB_{AMFM} = IB_{AM} + IB_{FM} \tag{10}$$

Fig. 3 Illustration of AMFM model decomposition. **a** IB of the AMFM; **b** IB of the FM; **c** IB of the AM

Next, we'll focus on how to estimate $P_k(t)$ and $Q_k(t)$. From $P_k(t) = a_k(t) \exp \left(j2\pi(f_k(t) - \hat{f}_k(t))t \right)$, we can see that $\hat{f}_k(t) \Rightarrow f_k(t)$, then, $P_k(t) \Rightarrow a_k(t)$. When $\hat{f}_k(t) = f_k(t)$, $P_k(t)$ has the least volatility. Thus, we can convert the signal decomposition problem into the following optimization problem:

$$
\min_{\{P(t),\hat{f}(t)\}} \left\{ \sum_{k=1}^{K} \|T(P_k(t))\|_2^2 \right\},
$$
$$
s.t. \ \left\| x_A(t) - \sum_{k=1}^{K} P_k(t) \cdot Q_k(t) \right\|_2^2 \leq \varepsilon, \tag{11}
$$

where ε is the noise components in signal, T is a differential operator which is used to minimize the amplitude of the signal. In this paper, the second-order differential operator is chosen as T, and the higher-order operator can also be used to detect the components with rapidly changing amplitudes.

The above optimization problem can be transformed into the corresponding Lagrange optimization equation:

$$
\Gamma(P_k, Q_k) = \sum_{k=1}^{K} \|T(P_k(t))\|_2^2 + \lambda \left(\left\| \sum_{k=1}^{K} P_k(t) * Q_k(t) - x_A(t) \right\|_2^2 \right), \tag{12}
$$

where λ is the Lagrange multiplier.

In addition, during the optimization of the equation, the most of the component $(s_{k_A}(t))$ is extracted from $x_A(t)$. However, we found that, a small portion of $s_{k_A}(t)$ is retained in the residual signal. In order to solve this problem, we learn from [21], using a less greedy approach to keep more information in the residual signal so that we can obtain a complete $s_{k_A}(t)$. Thus, we propose the following solution to the optimization problem:

$$
\Gamma(P_k, Q_k) = \sum_{k=1}^{K} \|T(P_k(t))\|_2^2 + \lambda \left(\left\| \sum_{k=1}^{K} P_k(t) * Q_k(t)(1 + \upsilon_k) - x_A(t) \right\|_2^2 \right), \tag{13}
$$

where λ is the Lagrange multiplier and υ_k is the leak factor of k-th component.

We obtain the optimal formula of $P_k(t)$ by the partial differential equations (PDEs) and alternating direction method of multipliers (ADMM):

$$
P_k(t) = \left(\frac{T^H T}{\lambda} + Q_k(t)^H Q_k(t)(1 + \upsilon_k)^2 \right)^{-1} Q_i(t)^H (1 + \upsilon_k)(x_A(t) - \sum_{K \neq k} P_k(t) \cdot Q_k(t)(1 + \upsilon_k)) \tag{14}
$$

where $Q_k(t) = \exp \left(j2\pi\hat{f}_k(t)t \right)$.

Next, we discuss how to implement the iterative formula of $Q_k(t)$. The definition of $Q_k(t)$ shows that the accuracy of component depends on the estimation of $\hat{f}_k(t)$, so we implement the iterative update of $\hat{f}_k(t)$ to achieve $Q_k(t)$ update. The

definition of $P_k(t)$ shows that the frequency error $(\Delta f_k(t))$ between $\hat{f}_k(t)$ and $f_k(t)$ is the phase of $P_k(t)$. Thus, the iterative formula for $\hat{f}_k(t)$ is:

$$\hat{f}_{k+1}(t) = \hat{f}_k(t) + \angle P_k(t) \tag{15}$$

where $\angle P_k(t)$ is the phase of $P_k(t)$.

The iterative formula of $Q_k(t)$ is:

$$\begin{aligned} Q_k(t) &= \exp\left(j2\pi\left(\hat{f}_k(t) + \Delta f_k(t)\right)t\right) \\ &= \exp\left(j2\pi\left(\hat{f}_k(t) + \angle P_k(t)\right)t\right) \end{aligned} \tag{16}$$

Therefore, the estimation of the k-th components is expressed as:

$$\hat{s}_k(t) = \mathrm{real}\left(P_k(t) \cdot Q_k(t)(1 + v_k)\right). \tag{17}$$

By comparing (7) and (14), it can be found that the iterative formula of $P_k(t)$ in multi-model signal decomposition is mainly embodied in $x_A(t)$ and $\left(x_A(t) - \sum_{K \neq k} P_k(t) \cdot Q_k(t)\left(1 + v_k\right)\right)$. From this we can see that the estimation of $P_k(t)$ is carried out by the signal without the other components. The advantages of this processing are as follows:

(1) Better exclusion of the influence of other components on the estimation of this component.
(2) For the cross-frequency part, the optimal allocation ratio of each component can be obtained by iterative calculation of different components in this region.
(3) The signal decomposition problem of multiple models can be degraded into the estimation problem of a single model.

In order to ensure the fast convergence of the algorithm, we need to realize the optimization formula of the parameters in the algorithm. There are two parameters of the algorithm to be optimized: the Lagrange multiplier (λ) and the leak factor (v_k). The leakage factor is that the component is not fully extracted and leaked part of the energy in the residue. It is described by formula as $x = \hat{s}_k + \hat{u}$, where $\hat{u} = \sum_{K \neq k} s_k + u$ consists of the noise u and residual components. Since the component is orthogonal to the residue, we obtain $\hat{s}_k(\hat{s}_k + u) = (1 + v_k)\hat{s}_k\hat{s}_k$. In addition, the components are directly independent of each other, so we can rewrite the upper form $\hat{s}_k\left(x - \sum_{K \neq k} P_k \cdot Q_k(1 + v_k)\right) = (1 + v_k)\hat{s}_k\hat{s}_k$. Then we can get the following iterative formula:

$$v_k(t) = \frac{\hat{s}_k(t)(x(t) - \sum_{K \neq k} P_k(t) \cdot Q_k(t)(1 + v_k))}{\hat{s}_k(t)\hat{s}_k(t)} - 1 \tag{18}$$

From the above analysis, we can see that the signal decomposition algorithm of multi-model can be converted into the estimation problem of single model by ADMM. And next, we'll introduce λ updated formula.

Parameter λ is a bridge to balance the objectives and constraints in the optimization equation. In addition, as the optimization equation advances, the second

part of the optimization formula (13) should be weakened, so λ should be gradually reduced. We embed (14) in (17) and get the following formula:

$$s_k(t) = \frac{Q_i(t)^H(1 + v_k)(x_A(t) - \sum_{K \neq k} P_k(t) \cdot Q_k(t)(1 + v_k)) \cdot Q_k(t)(1 + v_k)}{T^H T / \lambda + Q_k(t)^H Q_k(t)(1 + v_k)^2}$$

$$= \frac{\lambda}{T^H T / Q_k(t)^H Q_k(t)(1 + v_k)^2 + \lambda} \hat{s}_k(t) \qquad (19)$$

We define $O_k = T^H T / Q_k(t)^H Q_k(t)(1 + v_k)^2 + \lambda$, thus, $\lambda = s_k(t) / \hat{s}_k(t) \cdot O_k$. When $\hat{f}(t) \rightarrow f(t)$, $Q_i(t)$ approximates a stable exponential function. We can consider O_k to be a slowly varying value. Therefore, we can estimate the following equation:$\lambda_i / \lambda_{i+1} \approx \hat{s}_{i+1} / \hat{s}_i \approx 1 + v$. Thus, the estimated iteration formula of λ as:

$$\lambda_{i+1} = \frac{\lambda_i}{1 + \sum v_k}. \qquad (20)$$

3.2 IF Initialization

This algorithm runs on the premise of the estimated IF of components and then realizes the iterative update of the IA and IF of the components. There are many ways to estimate the IF of signal components, such as STFT, SET. However, accurate separation of component frequencies is an important problem for components with crossover frequency. This paper uses the Ridge path regrouping (RPRG) method to realize the ridge curve segmentation and extraction of crossover frequency [5]. The implementation of this algorithm is divided into the following steps:

(1) Calculate the time–frequency representation (TFR) of the multi-component signal, and then extract all the frequency ridges of the signal. This part can realize the TFR of the signal by STFT, and then obtain the IF ridges of all components in the form of the local extremum. We use SET to achieve IF of the ridge line. The TFR of SET with $s(t) = A \cdot \exp(jf_0 t)$ is expressed as $G(t,f) = A \cdot \hat{g}(f - \xi) \exp(jf_0 t)$. IF the representation described is $f_t(t,f) = -j\partial_t G(t,f) / G(t,f)$. And then the IF ridges (IFR) of the components is expressed as:

$$\text{IFR}_t(t,f) = \begin{cases} 1 & f_t(t,f) > 0.5\Delta\omega \\ 0 & \text{others} \end{cases} \qquad (21)$$

where $\Delta\omega$ is minimum resolution interval in frequency domain.

(2) Find all intersecting intervals for all overlapping ridge curves. Cross threshold for frequency to be defined, which is set to 3% of the sampling frequency.

(3) Recombine the ridges in each intersection interval. The ridge recombination is reconnected according to the rate of change of the ridge curve in this interval.

From the above description, it can be seen that the ridge extraction of overlapping frequency fully takes into account the amplitude and local extremum of the IF of the component. IFR segment reorganization decision is based on the change rate of each curve segment direction and the corresponding time–frequency position. The IFR of the components estimated by RPRG can satisfy both the smoothness of the IF and the actual conditions of the components.

3.3 Proposed Signal Decomposition Algorithm

This algorithm can realize the decomposition of multi-component signal through one processing and accurately estimate the model parameters of each component. The signal must be converted to a complex domain by HT before processing. Then, the initialization estimation of the IF ridges of each model is realized by RPRG in the TFR of the signal, and then $P_k(t)$ and $Q_k(t)$ of each model are initialized. Finally, the optimal solution of the model parameter is obtained by cyclic iteration. From the above description, we can see that the proposed algorithm can be regarded as a complex extension of VNCMD [4].

The processing flow of the proposed algorithm is as follows:

Algorithm: Proposed algorithm

Step1: The analytic signal of $x_A(t)$; and Initialize λ_i, υ_{k_0}, and topping threshold ε.

Step2: Calculation IFs ($\hat{f}_k(t)$) of each component by RPRG.

Step3: Initialize parameters for each model through the following formula.

$$\begin{cases} Q_{k_0}(t) = \exp(j2\pi\hat{f}_k(t)t) \\ P_{k_0}(t) = (T^H T/\lambda_i + Q_{k_0}(t)^H Q_{k_0}(t)(1+\upsilon_{k_0})^2)^{-1} Q_{k_0}(t)^H (1+\upsilon_{k_0})(x_A(t) - \sum_{K \neq k} P_k(t) \cdot Q_k(t)(1+\upsilon_k)) \end{cases}$$

Step4: Update model parameters $P_{k_i}(t)$ and $Q_{k_i}(t)$ by formulas (14) and (16), respectively.

Step5: Obtain the model components real($x_i(t)$) from formula (17).

Step6: Update iteration parameters λ_i and υ_{k_i}.

Step7: Updating IF by $\hat{f}_{k+1}(t) = \hat{f}_k(t) + \angle P_{k_i}(t)$.

Step8: If $\sum \|x_i(t) - x_{i-1}(t)\|_2^2 / \|x_i(t)\|_2^2 < \varepsilon$, then stop; else, go Step 4.

The parameters of multiple models in the algorithm need to be initialized; we give the initialization parameters as follows: $\lambda_i = 1e-5$, $\upsilon_{k_0} = 1e-2$ and $\varepsilon = 1e-7$. As the algorithm proceeds, these parameters will continuously approximate the optimal solution.

The complexity of this algorithm is mainly matrix calculation. Assuming that the length of the analyzed signal is n, thus, the matrix to be used in the algorithm is a two-dimensional matrix ($n \times n$). The computational complexity of the two-dimensional matrix is $O(n^{2.3728639})$ [12], and the computational complexity of the proposed algorithm is $O(m * n^{2.3728639})$, where m is the number of iterations.

Fig. 4 Extracted results of IF
by RPRG

(a)
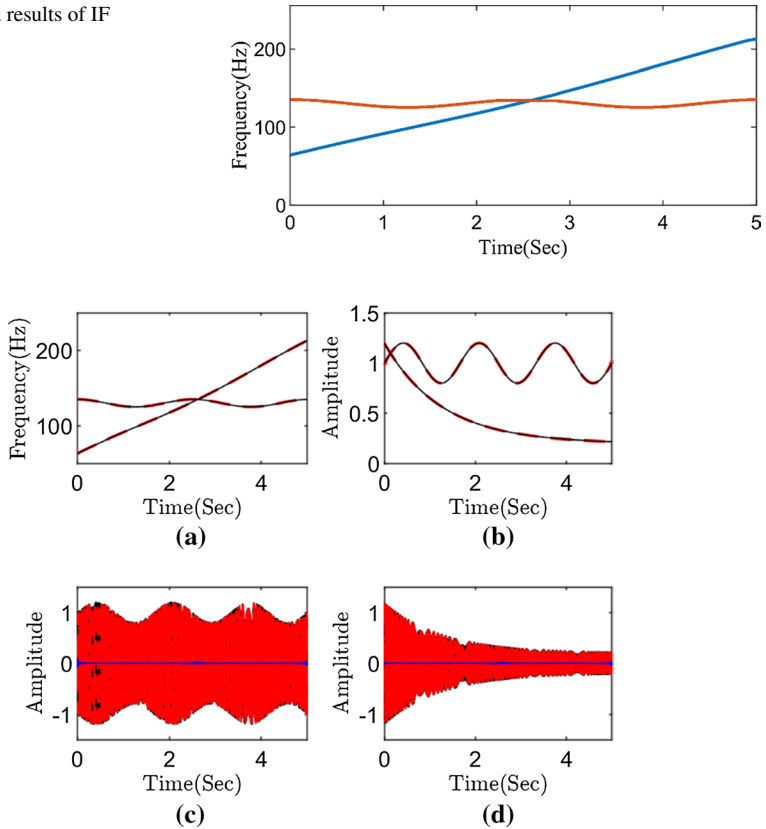
(b)

(c)

(d)

Fig. 5 Extracted results of signal (8) by the proposed method. **a** IFs of extracted models, **b** IAs of extracted models, **c–d** two extracted models by proposed method (Black line: the ideal waveform; red dotted line: the estimated information; blue line: estimated error) (Color figure online)

3.4 Performance Testing of the Algorithm

In this section, we demonstrate the decomposition performance of the proposed algorithm by analyzing signal (8). The reconstructed IF graph by RPRG is shown in Fig. 4. It can be seen from Fig. 4 that the IFs of the two components are accurately separated. The analysis results obtained by the proposed algorithm are shown in Fig. 5. Figure 5a–b shows the IAs and IFs information of the estimated models, respectively, and Fig. 5c–d shows the two reconstructed signal components, respectively. We can see from the detection results that the IFs and IAs of the two models are accurately estimated, and the two components can also be accurately segmented in the frequency crossover range. In addition, the error between the reconstructed component and the original component is very small, which indicates that the proposed algorithm can decompose the frequency cross signal model effectively.

To analyze the convergence performance of the algorithm, we introduce relative error (RE) as an evaluation index:

$$\text{RE} = \frac{\|\hat{s}(t) - s(t)\|_2}{\|s(t)\|_2}. \tag{22}$$

The RE trend diagram of the proposed algorithm in analyzing signal (8) is shown in Fig. 6. Figure 6a–b shows the RE of the estimated IF and the reconstructed components for each iteration, respectively. From the estimated results, it can be seen that the convergence rate of the IF is faster than that of the model. IFs calculation accuracy can reach 10^{-2} through several iterations, and the models need 100 iterations to achieve this accuracy.

4 Experiment

In this section, to verify the performance of the proposed algorithm, we will use some experiments for testing. These experimental signals include artificial signals and natural signals. And we also cite some excellent algorithms for contrast testing, such as VMD and ACMP. All the experiments in this paper are run under MATLAB R2018a with CPU Intel(R) Core(TM) i5-4460 and memory 8G on a personal computer.

4.1 Artificial Signals

We consider analyzing the time-varying signals consisted of three components, which as follows:

$$
\begin{aligned}
s(t) &= s_{m1}(t) + s_{m2}(t) + s_{m3}(t) \\
s_{m1}(t) &= (1 + 0.4\sin(2\pi \cdot 2t)) \cdot \sin\left(2\pi \cdot (0.23 + 80t + t^2)\right) \\
s_{m2}(t) &= (1 + 0.5\cos(2\pi \cdot 0.3t)) \cdot \sin\left(2\pi \cdot (150t - t^2 + 50\sin(0.25\pi t))\right) \\
s_{m3}(t) &= (0.6 + \exp(-0.8t)) \cdot \sin\left(2\pi \cdot (150t + 0.2t^2 - 45\sin(0.25\pi t))\right)
\end{aligned}
\tag{23}
$$

The sampling frequency of the signal is 512 Hz, and the signal is sampled for 15 s. The signal waveform is shown in Fig. 7, where Fig. 7a shows the waveform

Fig. 6 Convergence trend of the model during algorithm iteration. **a** RE of IFs iterative trends, **b** RE of model iterative trends
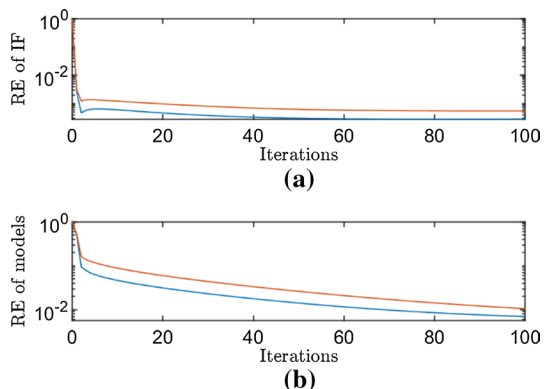
Fig. 7 Information of the artificial signals in 4.1. **a** Waveform of the s; **b–d** Waveform of s_{m1}–s_{m3}
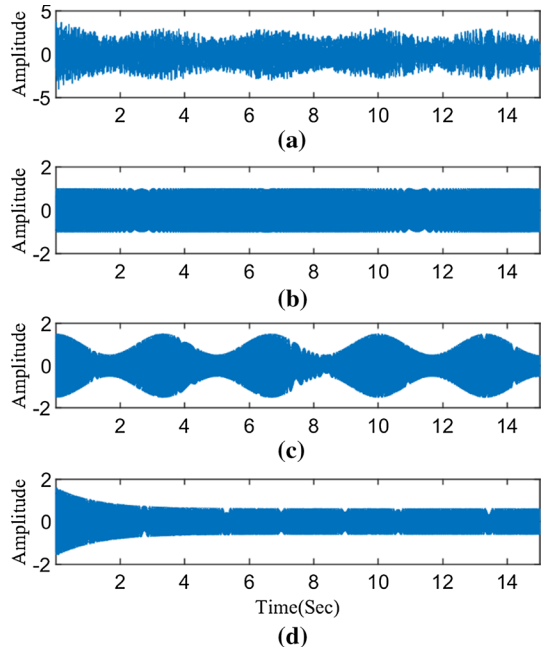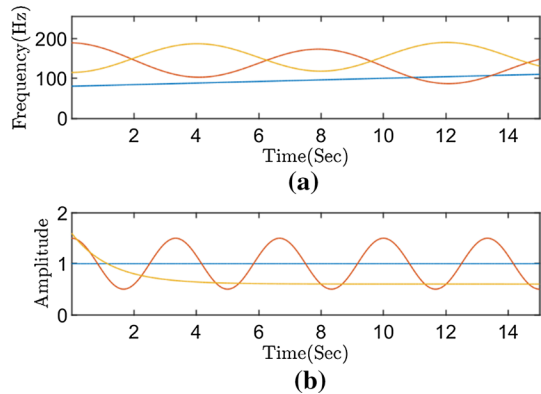

Fig. 8 Information of the components in 4.1. **a** IFs of three components in signal; **b** IAs of three components in signal

of $s(t)$ and Fig. 7b–d is the waveform of three components in $s(t)$. The tracks of IFs and IAs of the three components are shown in Fig. 8. It can be seen that the signal is composed of three components, and each component is under the AMFM model. Besides, the components are crossed in multiple places in the frequency domain (such as 1.9 s, 6.2 s, 9.6 s, 10.9 s, 13.4 s, 14.6 s, etc.).

We first use the proposed algorithm to decompose the signal into three sub-components and estimate the IA and IF parameters of each component. The decomposition results are shown in Figs. 9, 10. From the decomposition results, we can see that the proposed algorithm can accurately estimate the IF and IA of each component, even at the frequency overlap. By comparing the error waveform of each

Fig. 9 Extracted results of the signal in (23) using proposed method. **a** IFs of Extracted components, **b** IAs of Extracted components (black line: the ideal waveform; red dotted line: the estimated information) (Color figure online)
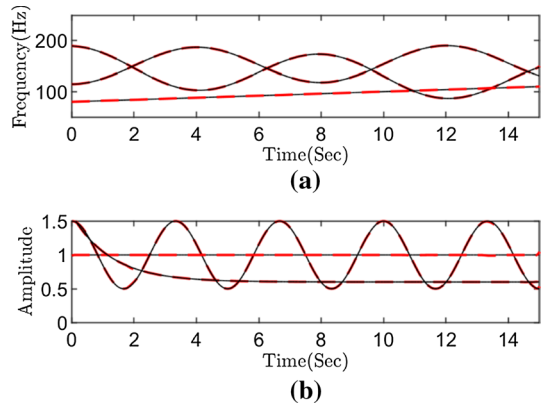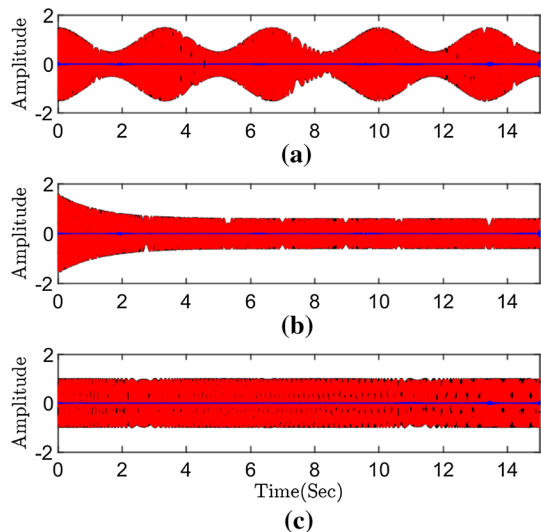

(a)

(b)

Fig. 10 Results of the reconstructed component using proposed method. **a** The first extracted component, **b** the second extracted component, **c** the third extracted component (black line: the ideal waveform; red dotted line: the estimated information; blue line: estimated error) (Color figure online)

(a)

(b)

(c)

component, it can be seen that the proposed algorithm can accurately reconstruct each component of the signal.

Moreover, we employ VMD and ACMP algorithms to decompose the signal, and the decomposition results are shown in Fig. 11. Figure 11a1–a3 shows the three extracted components of the signal by VMD, and Fig. 10b1–b3 shows the extracted results of ACMP. From extracted results, we can find that there is a serious spectrum aliasing phenomenon in the decomposition results of the VMD. ACMP can decompose three components of the signal, but there are obvious detection errors at the intersection of IFs, such as 6.2 *s* and 10.9 *s* of Fig. 11b1, 1.9 *s* and 14.6 *s* of Fig. 11(b2), 10.9 *s* and 13.4 *s* of Fig. 11b3.

Now, we quantify the accuracy of each decomposition algorithm by RE. The RE results for each algorithm are shown in Table 1. From Table 1, we can see that the
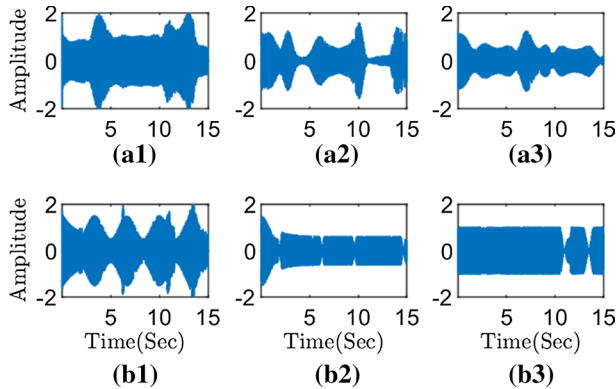
Fig. 11 Comparison experiment for model extraction. **a1–a3** Extracted models by VMD, **b1–b3** extracted models by ACMD

RE accuracy of the proposed method can reach the number level of 10^{-3} when the frequency crossover signal is decomposed, which is much higher than that of VMD and ACMD.

4.2 Natural Signals: Bat Signal

The analysis of natural signals is the most effective method to verify the performance of the algorithm. The bat signal is selected in this experiment to test the performance of the proposed algorithm [1]. The signal is sampled at intervals of 7 μs and continuously collected 0.0028 s. The waveform and spectrum of the collected bat signal are shown in Fig. 12. From Fig. 12, it can be seen that the bat signal is composed of multiple components, three of which reflect strong energy in the spectrum, and there is a weak time-varying component in the upper right corner of the spectrum.

This experiment will extract the components of the signal by the proposed algorithm and estimate their parameters. The extracted results are shown in Fig. 13, which contains the waveform and spectrum information of the extracted components, as well as the IF and IA variation trends of each component. From the results of the extracted components, it can be seen that all the extracted components have time-varying amplitude and frequency. The energy concentration points of each component are clearly distinguished, and each component does not cover the whole-time interval. By comparing the spectrum, we can find that the extracted spectrum

Table 1 Comparison experiment for model extraction with the proposed method and some publications

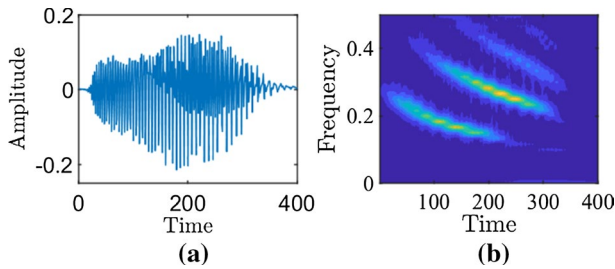| Methods	VMD	ACMD	Proposed method
s_{m1}	$5.34*10^{-1}$	$6.06*10^{-1}$	$8.00*10^{-3}$
s_{m2}	$8.38*10^{-1}$	$7.90*10^{-1}$	$8.50*10^{-3}$
s_{m3}	$9.90*10^{-1}$	$2.87*10^{-1}$	$5.90*10^{-3}$

Fig. 12 Waveform and spectrum of the bat signal. **a** The waveform of the bat signal; **b** spectrum of the bat signal
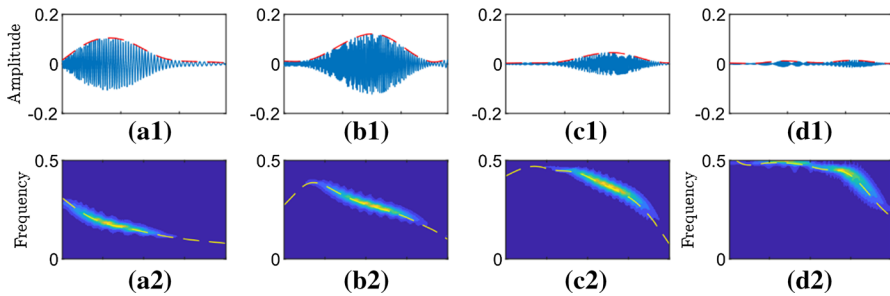

Fig. 13 Decomposed results of bat signal by proposed method. **a1–d1** Waveform of extracted components; **a2–d2** corresponding spectrum of a1-d1 (red dotted line: the estimated information of IA; yellow dotted line: the estimated information of IF) (Color figure online)

information of each component is consistent with the spectrum distribution of the original signal, which also reflects the effectiveness of the proposed algorithm.

4.3 Natural Signals: Voice of Humpback Whale

The ocean is vast and contains countless creatures. The ocean signals we obtained through sensors often contain strong interference components. In this experiment, we use the proposed algorithm to analyze the voice of the humpback whales from the ocean, which contains high interference noise. The humpback whale's voice is recorded off the coast of San Francisco, California, and the humpback whale's voice is usually aimed at finding mates and breeding offspring [9].

This signal was continuously collected at a sampling frequency of 11.025 kHz for 13.48 s, the waveform of which is shown in Fig. 14o. It can be seen from the figure that the signal consists of a total of 4 segments. In this experiment, we first intercept the four-segment signal and decompose the sub-signal separately by the proposed algorithm. The estimated IF contained in each segment signal is shown in Fig. 14a–d by the proposed algorithm in this paper, and the waveforms and estimated IAs of each component are shown in Fig. 15.
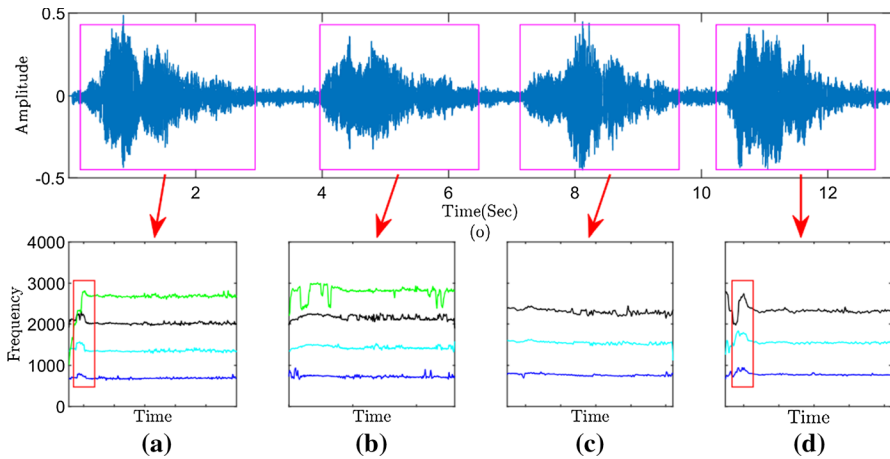
Fig. 14 Waveform of voice of humpback whale and decomposed IFs results by the proposed algorithm. **o** The waveform of signal; **a–d** the estimated IFs results of each component by the proposed algorithm

From the decomposition results, it can be seen that the first two components are composed of four components, and the last two components are composed of three components. These components all contain spectrum components of 0.67 kHz, 1.35 kHz and 2.20 kHz, while the first two-segmented signals also contain 2.8 kHz frequency components with less energy. Hence, we can explain that the component of 2.8 kHz is missing in the ambient noise due to the distance between the sensor and the sound source. So, we mainly analyze the characteristics of the three
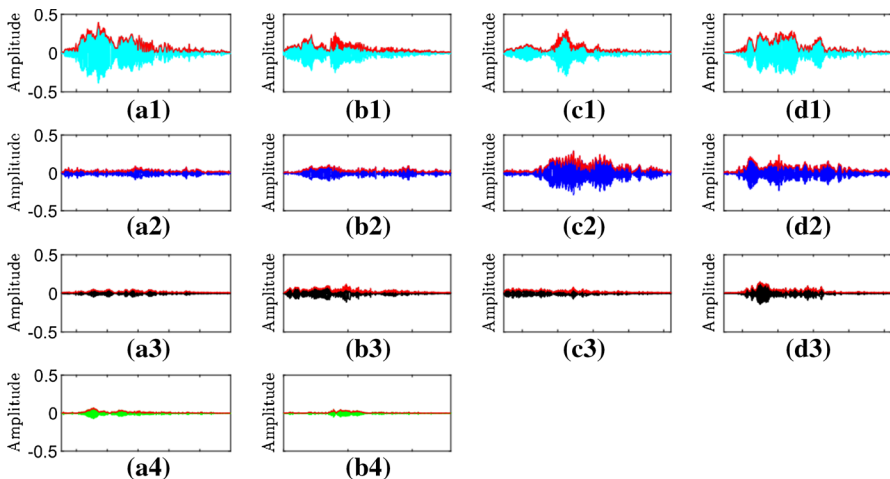

Fig. 15 Decomposed results of voice of humpback whale by the proposed algorithm. **a1–a4** Waveform of extracted components from the first segment signal; **b1–b4** Waveform of extracted components from the second segment signal; **c1–c3** Waveform of extracted components from the third segment signal; **d1–d3** Waveform of extracted components from the forth segment signal (red line: the estimated information of IA) (Color figure online)

components with strong energy. We know that the characteristics of the signal are mainly reflected in the frequency and the energy of each frequency band. By analyzing the IF information of the signal, we can clearly find that the first segment and the fourth segment signal have an obvious IF jump phenomenon at the beginning stage of the component. And the IF of the second and the third segments tends to be balanced. So, we can confirm that the first and the fourth segments of the signal are made by the same humpback whale, while the second and the third are made by another whale.

4.4 Natural Signals: Speech Signal

Generally speaking, the speech signals can be modeled as the sum of AMFM models. In this experiment, we use the proposed algorithm to decompose the digitalized sound of the word, /gao/ [26]. This speech signal is continuously collected 0.47 *s* at 11.025 kHz digitization, the waveform and spectrum of which are shown in Fig. 16a–b. As can be seen from Fig. 16b, the speech signal has multiple principal components, and the instantaneous frequency fluctuation of each component is not obvious, which accords with the AMFM model. The waveform of the four extracted
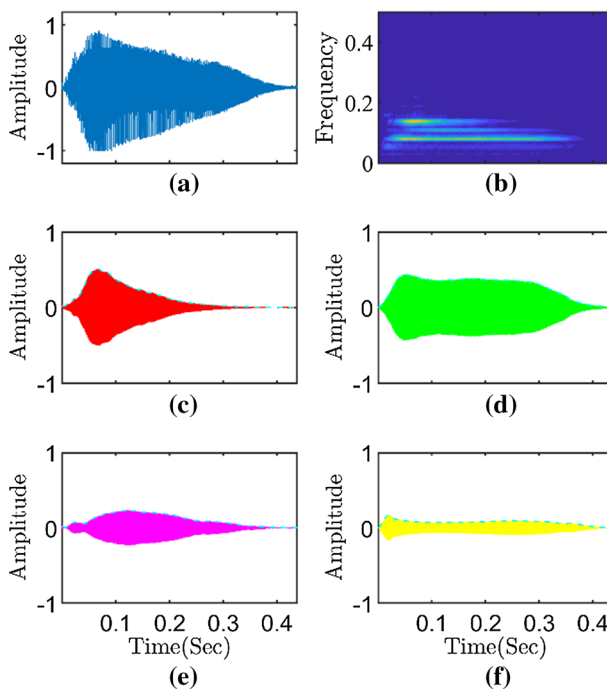

Fig. 16 Information of the speech signal and extracted results by the proposed method. **a** The waveform of the speech signal; **b** spectrum of the speech signal; **c** the first extracted component; **d** the second extracted component; **e** the third extracted component; **f** the fourth extracted component (cyan dotted line: extracted IA)

Fig. 17 Decomposed results of the speech signal by proposed method. **a** The extracted IFs information in the spectrum of the speech signal; **b** the extracted IAs information (red line: the first extracted component; green line: the second extracted component; magenta line: the third extracted component; yellow line: the fourth extracted component) (Color figure online)
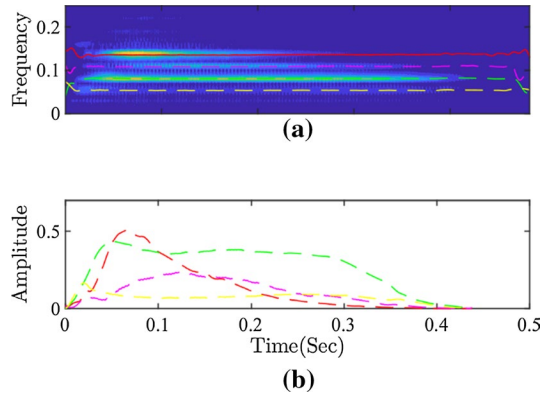
components are shown in Fig. 16c–f, and the IAs and IFs of the extracted components are shown in Fig. 17.

The estimated results of the IAs of each component are consistent with the start and end times of the component. At the same time, we can see that the IF and IA of each component are consistent with the time–frequency distribution characteristics of the signal. Moreover, the first two extracted components represent the /g/ and /ao/ of Chinese pronunciation, respectively. We can see from this experiment that the algorithm is effective in speech signal decomposition.

5 Conclusions

In this paper, a multi-component signal decomposition algorithm based on the complex-AMFM model is presented. By the proposed algorithm, the signals with multiple components can be decomposed into the sum of multiple AMFM models at a time, and the parameters of each model can be accurately estimated. Besides, this algorithm also has a good decomposition effect on the phenomenon of frequency crossover. We compare the proposed algorithm with the excellent signal decomposition algorithms in the industry (i.e., VMD, ACMD) to verify the performance of the proposed algorithm. By experimental verification, the RE of the proposed method can reach 10^{-3} levels when analyzing the frequency crossover signal, which is much higher than that of other algorithms. In addition, the effectiveness of the proposed algorithm is verified by many examples of real speech signals (i.e., bat, humpback whale and humans). Due to the need to transform the signal into the analytic domain, the noise resistance of the algorithms is weak, which is the focus of our next research.

Data availability The data that support the findings of this study are available from the corresponding author on request.

References

1. Bat. https://cpb-us-e1.wpmucdn.com/blogs.rice.edu/dist/0/7717/files/software/batsignal.zip.
2. E. Bedrosian, A product theorem for Hilbert transform. Proc. IEEE **51**(5), 868–869 (1963). https://doi.org/10.1109/PROC.1963.2308
3. C.Y. Chen, S.M. Guo, W.S. Chang et al., An improved bidimensional empirical mode decomposition: a mean approach for fast decomposition. Signal Process. **98**, 344–358 (2014). https://doi.org/10.1016/j.sigpro.2013.11.034
4. S.Q. Chen, X.J. Dong, Z.K. Peng et al., Nonlinear chirp mode decomposition: a variational method. IEEE Trans. Signal Process. **65**(22), 6024–6037 (2017). https://doi.org/10.1109/TSP.2017.2731300
5. S.Q. Chen, X.J. Dong, G.P. Xing et al., Separation of overlapped non-stationary signals by ridge path regrouping and intrinsic chirp component decomposition. IEEE Sens. J. **17**, 5994–6005 (2017). https://doi.org/10.1109/JSEN.2017.2737467
6. S.Q. Chen, Y. Yang, Z.K. Peng et al., Adaptive chirp mode pursuit: algorithm and applications. Mech. Syst. Signal Process. **116**(1), 566–584 (2019). https://doi.org/10.1016/j.ymssp.2018.06.052
7. I. Daubechies, J.F. Lu, H.T. Wu, Synchrosqueezed wavelet transforms: an empirical mode decomposition-like tool. Appl. Comput. Harmon. Anal. **30**(2), 243–261 (2011). https://doi.org/10.1016/j.acha.2010.08.002
8. L. Debnath, *Wavelet Transforms and Their Applications* (Springer, Birkhäuser, 2002)
9. Discovery of Sound in the Sea. 2002. [Online]. Available: https://dosits.org/resources/resource-categories/feature-sounds/haunting-refrains-humpback/.
10. K. Dragomiretskiy, D. Zosso, *Two-Dimensional Variational Mode Decomposition* (Springer, Cham, 2015), pp. 197–208
11. K. Dragomiretskiy, D. Zosso, Variational mode decomposition. IEEE Trans. Signal Process. **62**(3), 531–544 (2014). https://doi.org/10.1109/TSP.2013.2288675
12. F.L. Gall. Powers of tensors and fast matrix multiplication. Proceedings of the 39th International Symposium on Symbolic and Algebraic Computation. 296–303 (2014). https://doi.org/10.1145/2608628.2608664.
13. Q.W. Gao, D. Zhu, D. Sun et al., A denoising method based on null space pursuit for infrared spectrum. Neurocomputing **137**, 180–184 (2014). https://doi.org/10.1016/j.neucom.2013.04.057
14. B.K. Guo, S.L. Peng, X.Y. Xu, Complex-valued differential operator-based method for multi-component signal separation. Signal Process. **132**, 66–76 (2017). https://doi.org/10.1016/j.sigpro.2016.09.015
15. X.Y. Hu, S.L. Peng, W.L. Hwang, Adaptive integral operators for signal separation. IEEE Signal Process. Lett. **22**(9), 1383–1387 (2015). https://doi.org/10.1109/LSP.2014.2352340
16. X.Y. Hu, S.L. Peng, W.L. Hwang, Multicomponent AM-FM signal separation and demodulation with null space pursuit. Signal, Image Video Process. **7**, 1093–1102 (2013). https://doi.org/10.1007/s11760-012-0354-9
17. X.Y. Hu, S.L. Peng, W.L. Hwang, Operator based multicomponent AM-FM signal separation approach. IEEE Int. Workshop Mach. Learn. Signal Process. **18**, 1–6 (2011). https://doi.org/10.1109/MLSP.2011.6064592
18. N.E. Huang, Z. Shen, S.R. Long et al., The empirical mode decomposition and the Hilbert spectrum for nonlinear and non-stationary time series analysis. Proc. Math. Phys. Eng. Sci. **454**, 903–995 (1998). https://doi.org/10.1098/rspa.1998.0193
19. T. Liu, Z.J. Luo, J.H. Huang et al., A comparative study of four kinds of adaptive decomposition algorithms and their applications. Sensors **18**(7), 1–51 (2018). https://doi.org/10.3390/s18072120
20. F.J. Owens, M.S. Murphy, A short-time Fourier transform. Signal Process. **14**(1), 3–10 (1988). https://doi.org/10.1016/0165-1684(88)90040-0
21. S.L. Peng, W.L. Hwang, Null space pursuit: an operator-based approach to adaptive signal separation. IEEE Trans. Signal Process. **58**(5), 2475–2483 (2010). https://doi.org/10.1109/TSP.2010.2041606

22. D.H. Pham, S. Meignen, High-order synchrosqueezing transform for multicomponent signals analysis-with an application to gravitational-wave signal. IEEE Trans. Signal Process. **65**(12), 3168–3178 (2019). https://doi.org/10.1109/TSP.2017.2686355

23. C. Rader, The fast Fourier transform. IEEE Trans. Acoust. Speech Signal Process. **23**(2), 245–246 (1975). https://doi.org/10.1109/TASSP.1975.1162674

24. N. Rehman, H. Aftab, Multivariate variational mode decomposition. IEEE Trans. Signal Process. **67**(23), 6039–6052 (2019). https://doi.org/10.1109/TSP.2019.2951223

25. X.T. Tu, Y. Hu, F.C. Li et al., Demodulated high-order synchrosqueezing transform with application to machine fault diagnosis. IEEE Trans. Industr. Electron. **66**(4), 3071–3081 (2019). https://doi.org/10.1109/TIE.2018.2847640

26. Voice signal /gao/ [EB/OL]. https://hanyu-word-pinyin-short.cdn.bcebos.com/gao1.mp3.

27. Y.X. Wang, F.Y. Liu, Z.S. Jiang et al., Complex variational mode decomposition for signal processing applications. Mech. Syst. Signal Process. **86**, 75–85 (2017). https://doi.org/10.1016/j.ymssp.2016.09.032

28. Z.H. Wu, N.E. Huang, Ensemble empirical mode decomposition: a noise-assisted data analysis method. Adv. Adapt. Data Anal. **01**(01), 1–41 (2009). https://doi.org/10.1142/S1793536909000047

29. J.R. Yeh, J.S. Shieh, N.E. Huang, Complementary ensemble empirical mode decomposition: a novel noise enhanced data analysis method. Adv. Adapt. Data Anal. **02**(02), 135–156 (2010). https://doi.org/10.1142/S1793536910000422

30. G. Yu, Z.H. Wang, P. Zhao, Multisynchrosqueezing transform. IEEE Trans. Industr. Electron. **66**(7), 5441–5455 (2019). https://doi.org/10.1109/TIE.2018.2868296

31. G. Yu, M.J. Yu, C.Y. Xu, Synchroextracting transform. IEEE Trans. Industr. Electron. **64**(10), 8042–8054 (2017). https://doi.org/10.1109/TIE.2017.2696503

32. D. Zhu, Q.W. Gao, Y.X. Lu et al., A signal decomposition algorithm based on complex AM-FM model. Digit. Signal Processing. **107**, 1–9 (2020). https://doi.org/10.1016/j.dsp.2020.102860

33. D. Zhu, Q.W. Gao, D. Sun et al., A detection method for bearing faults using null space pursuit and S transform. Signal Process. **96**, 80–89 (2014). https://doi.org/10.1016/j.sigpro.2013.04.019

34. D. Zhu, Q.W. Gao, D. Sun et al., A detection method for bearing faults using complex-valued null space pursuit and 1.5-dimensional teager energy spectrum. IEEE Sens. J. **20**(15), 8445–8454 (2020). https://doi.org/10.1109/JSEN.2020.2983261

Publisher's Note Springer Nature remains neutral with regard to jurisdictional claims in published maps and institutional affiliations.

Authors and Affiliations

De Zhu[1] ⬛ **· Qingwei Gao[2] · Yixiang Lu[2] · Dong Sun[2]**

De Zhu
zhude@ahu.edu.cn

Yixiang Lu
lyxahu@126.com

Dong Sun
sundong@ahu.edu.cn

1 School of Computer Science and Technology, Anhui University, Hefei 230601, China

2 School of Electrical Engineering and Automation, Anhui University, Hefei 230601, China